ELSEVIER

Earth and Planetary Science Letters 199 (2002) 403–413

EPSL

www.elsevier.com/locate/epsl

Delayed cooling of the Earth's mantle due to variable thermal conductivity and the formation of a low conductivity zone

Arie P. van den Berg [a,*], David A. Yuen [b]

[a] *Department of Theoretical Geophysics, Institute of Earth Sciences, Utrecht University, 3508 TA Utrecht, The Netherlands*
[b] *Department of Geology and Geophysics and Minnesota Supercomputer Institute, University of Minnesota, Minneapolis, MN 55455, USA*

Received 22 October 2001; received in revised form 7 February 2002; accepted 8 February 2002

Abstract

The thermal conductivity of mantle materials decreases with higher temperatures and increases with greater pressure due to phonon mechanism, but increases with temperature for radiative transfer. This trade-off attribute allows for the formation of a low conductivity zone (LCZ) within the top thermal boundary layer in mantle convection. We have studied with a two-dimensional (2-D) cartesian model the potential of this low conductivity zone in retarding secular cooling of the mantle for a longer period of time than models with constant thermal conductivity. Using a recently proposed model for thermal conductivity and an adiabatic boundary condition for the bottom of the mantle, we have carried out a set of numerical experiments within the framework of the extended Boussinesq approximation for constant viscosity, depth-dependent thermal expansivity and variable thermal conductivity with surface Rayleigh numbers between around 10^6 and around 10^7. We have employed internal heating between two and four times the chondritic level and half-life time values of 2.5 Ga and 5 Ga. The cooling rate of the mantle can be decreased by the feedback interaction between mantle conductivity and internal heating, which gives rise to slower sinking cold currents. The retardation time increases with the strength of radiogenic heating and can be as long as a couple of billion years for high initial heating rates, four times the chondritic value. However, increasing the radiative contribution of the conductivity speeds up the cooling process. The less the radiative contribution is, the more mantle cooling would be retarded. In the course of adiabatic cooling we find the paradoxical situation in which the effective Rayleigh number of the mantle can actually increase with time. We suggest then that, because of the possibilities for the formation of low conductivity zones adjacent to the thermal boundary layers, which bring forth unexpected consequences, mantle thermal conductivity should be considered as a fundamentally important factor in constraining the thermal evolution of both the core and mantle.

Keywords: secular variations; cooling; thermal conductivity; mantle; convection; thermal history

1. Introduction

Secular cooling of the entire planet by mantle convection is an issue of central importance not only for mantle dynamics but also for the energetics of the geodynamo. Many factors influence

* Corresponding author. Tel.: +31-30-253-5031; Fax: +31-30-253-5030.
E-mail addresses: berg@geo.uu.nl (A.P. van den Berg), davey@krissy.msi.umn.edu (D.A. Yuen).

0012-821X/02/$ – see front matter
PII: S0012-821X(02)00531-9

the cooling history of the mantle. They include the initially hot formation and the temperature rise due to gravitational separation of the core from the mantle [1,2], the amount of ohmic dissipation in the outer core from dynamo action and the amount of radioactivity in the mantle and their effective decay time [3]. Secular cooling also has a direct impact on the formation of continental crust and mantle roots, since these processes depend critically on the temperature in the upper mantle [4]. Other dynamical processes which depend on secular cooling include the transition in the style of mantle convection with decreasing Rayleigh number in the presence of an endothermic phase transition [5] and rheological transition from non-Newtonian to Newtonian creep with decreasing convective vigor [6].

Recently Hofmeister [7,8] has introduced a new semi-empirical model of thermal conductivity, based on infrared spectroscopy and solid-state physics of phonons. One of the interesting physical attributes of mantle thermal conductivity is the well-known experimental fact [9] that conductivity from phonon mechanism decreases with temperature and increases with pressure, in the same manner as mantle viscosity. This property involving the trade-off between the temperature and pressure derivatives of the material property makes it possible for a low thermal conductivity zone to develop in the upper mantle, in the same manner as the well-known asthenosphere. The presence of a low conductivity zone allows for some feedback to take place in the presence of heating of any sort, be it radiogenic heating on a global basis or local viscous dissipation [10]. The purpose of this work is to demonstrate that the secular cooling of the Earth's mantle could be delayed by the presence of a low conductivity zone generated by mantle convection due to non-linear interaction caused by the temperature-dependence of mantle thermal conductivity and time-dependent radiogenic heating in the mantle. In van den Berg et al. [11] we have presented results showing the influence of variable conductivity in keeping the lower mantle very hot, leading to potentially melting scenarios today. Our results below will demonstrate that variable thermal conductivity may possibly exert a profound influence on balancing delicately the amount of heat generated in the outer core by ohmic dissipation from geodynamo fluid dynamics and the amount of radioactive heating in the mantle.

2. Model description

We have employed a thermal conductivity model [7,8] based on thermodynamic properties and supported by vibrational spectroscopy of mantle materials in the solid-state phase. We have applied this conductivity model to the olivine portion of the upper mantle. Therefore no crustal constituents are considered. Both temperature (T) and pressure (P) dependences are included in this model. The functional dependence of this conductivity model [7] takes the form:

$$k(T,P) = k_0(298/T)^a \exp[-(4\gamma + 1/3)\alpha(P)(T-298)]\left(1 + \frac{K_0' P}{K_0}\right) + \sum_{i=0}^{3} f b_i T^i \qquad (1)$$

where $k_0 = 4.7$ W K^{-1} m^{-1}, temperature T in Kelvin, the Grüneisen parameter, $\gamma = 1.2$, the phonon fitting parameter $a = 0.3$ characteristic of silicates, the bulk modulus $K_0 = 261$ GPa and its pressure derivative $K_0' = 5$, characteristic of lower mantle silicates. The constants b_i of the radiative term are obtained from least-squares fitting [7] and f is a fitting parameter, where $f = 1$ corresponds to the values given in [7] and values greater than 1 are used to mimick greater amounts of radiative conductive transfer. Effects of varying the parameter f have been demonstrated on controlling the time-dependence of mantle flow in both 2-D and 3-D simulations [12]. We note that the temperature derivative of the radiative thermal conductivity is positive, in contrast to the negativity of the temperature derivative of the phonon portion of the thermal conductivity. This difference will make a sharp impact on the cooling process of the mantle. We have employed a pressure-dependent thermal expansivity [13] which is parameterized by an algebraic function with the depth and decreases by a factor of 5 across the mantle [14].

The radiative contribution, which is non-linear in T, is given by the coefficients b_i in Eq. 1, which have been derived by fitting the spectroscopic data to the overtones [7]. Aside from the radiative contribution and the exponential dependence in temperature, the Hofmeister thermal conductivity model has temperature- and pressure-dependences, which behave similarly to the older thermal conductivity model [9] used in lithosphere–asthenosphere modelling [15].

We have used the thermal convection equations associated with the extended Boussinesq approximation [16]. A box with an aspect ratio of 2.5 has been chosen. For the boundary conditions, impermeable, free slip boundary conditions have been used for the velocity fields. For the thermal boundary conditions, we have imposed a temperature of 273 K at the top surface and zero heat-flux along the vertical boundaries. The initial temperature at the core–mantle boundary is set to 3773 K. In order to focus on the effects of secular cooling from 2-D high Rayleigh number convection, we have applied an adiabatic (zero heat-flux) boundary condition at the base of the mantle. An exponentially decaying heating term with a half-life of 2.5 Gyr has been used in the main. The amount of internal heating will be varied to monitor its interaction with the variable thermal conductivity. The viscosity is assumed to be constant, the thermal expansivity is pressure (depth)-dependent [13] and a thermal conductivity, the main objective in this study, which depends on both temperature and pressure, as given by Eq. 1 is used. A surface dissipation number $Di = \alpha g h / c_p$ of 0.47 is used throughout, where h is the mantle thickness, α is the surface value of the thermal expansivity, and c_p is the specific heat, taken to be 1.25 kJ kg^{-1} K^{-1}. The length scale has been non-dimensionalized by the mantle depth h, taken here to be 3000 km and the dimensionless time by the thermal diffusion time across this mantle depth. We have varied the surface Rayleigh number, which is based on the surface values of the physical parameters. Between 100×100 and 200×200 variably spaced grid points have been used in a finite-element code [17].

The non-linear time-dependent equation of the temperature has been integrated in time by a second order predictor–corrector scheme with a Picard iteration at each time step. Direct solvers are used to solve the resulting algebraic equations. The non-linear temperature equation in the extended Boussinesq setup is given in the dimensionless form:

$$\frac{\mathrm{D}T}{\mathrm{D}t} = \kappa(T,P)\nabla^2 T + \frac{\partial \kappa(T,P)}{\partial T}(\nabla T)^2 + \frac{\partial \kappa(T,P)}{\partial P}\frac{\partial P}{\partial z}\frac{\partial T}{\partial z} + \alpha(z) Di w (T + T_0) + \frac{Di}{Ra_s}\Phi + RH(t) \quad (2)$$

The vertical velocity is denoted by w and the dimensionless surface temperature by T_0. Viscous dissipation is given Φ, which represents the contraction between the deviatoric stress tensor and the strain rate tensor. The thermal diffusivity $\kappa(T,P)$ is given by $k(T,P)/\rho c_p$, where both ρ and c_p are assumed to have constant properties in our present level of approximation. The initial radiogenic strength is given by the non-dimensional heating number R [18] and the exponential decay rate $H(t)$. Higher spatial resolution than for constant conductivity is needed because of the nature of the additional terms in the energy equation, Eq. 2, which have three new non-linearities coming from the divergence of the heat-flux vector [19,20].

3. Results

For each case we have employed the same hot initial condition, which has been taken from a long-term statistically equilibrated solution with a high constant internal heating of $R = 40$ and a surface Rayleigh number $Ra_s = 8\times10^6$ and a variable thermal conductivity with an enhanced radiative conductivity of $f = 4.7$ [11,20]. The solutions shown below, unless otherwise indicated, are based on the usage of the thermal conductivity with $f = 1$ in Eq. 1. Fig. 1 shows two snapshots of the laterally varying portion of the thermal conductivity field, $\delta k(x,z)$, in which the horizon-

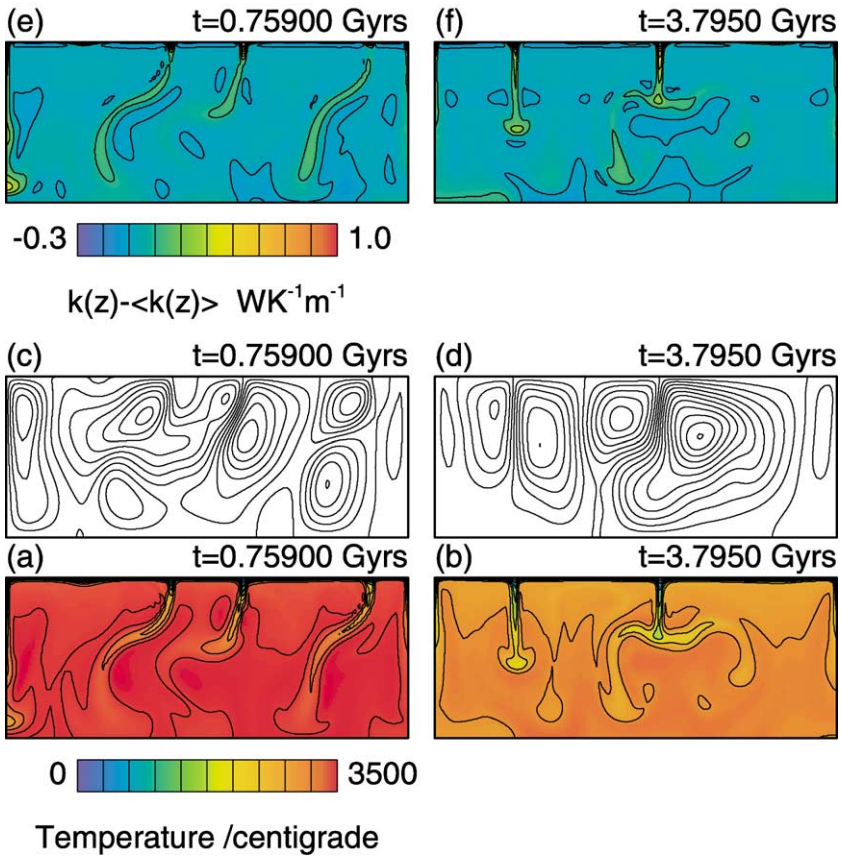

Fig. 1. Snapshots of the temperature field (bottom row), stream function (middle row) and corresponding lateral variation of the thermal conductivity field (top row), for two different time steps far apart: $t = 0.76$ Gyr and $t = 3.8$ Gyr after the start of the model calculation. The surface Rayleigh number $Ra_s = 8 \times 10^6$. The stream function contour spacing is 25 non-dimensional units. Velocity has been non-dimensionalized with respect to thermal diffusion time, based on the surface value of the conductivity. Color bars are given to show the range in both the temperature and lateral variations in the thermal conductivity field. The conductivity of cold downwellings is greater than the surrounding hot interior, whose conductivity (green-blue) is lower.

tally averaged conductivity has been subtracted from the total $k(x,z)$, the streamlines, and the temperature fields $T(x,z)$. The frames are taken at time frames 0.75 Gyr and 3.8 Gyr after the initial conditions. The surface Rayleigh number is 8×10^6 with an initial internal heating strength of $R = 20$ and the heating decays exponentially with a half-life time of 2.5 Gyr. We note that $R = 12$ would correspond to about the chondritic heating value commonly assumed for the entire mantle. The streamlines show that downwellings dominate the flow, as to be expected from the strong internal heating and penetrative convection prevailed initially [21] before settling into large-scale flow patterns more in line with whole mantle circulation. The secular cooling process from the adiabatic boundary condition is quite evident from comparing the two temperature fields. We can also discern the concentration of high conductivity in the cold limbs, which causes greater degree of thermal assimilation [22] and the low conductivity with the hot interior. The lateral variations in the conductivity field, in turn, will influence the global heat transport. Since the local temperature field and the conductivity depend on the magnitude of internal heating, such an interaction and its consequence on the evolution of the Earth's heat budget will form the basis of this

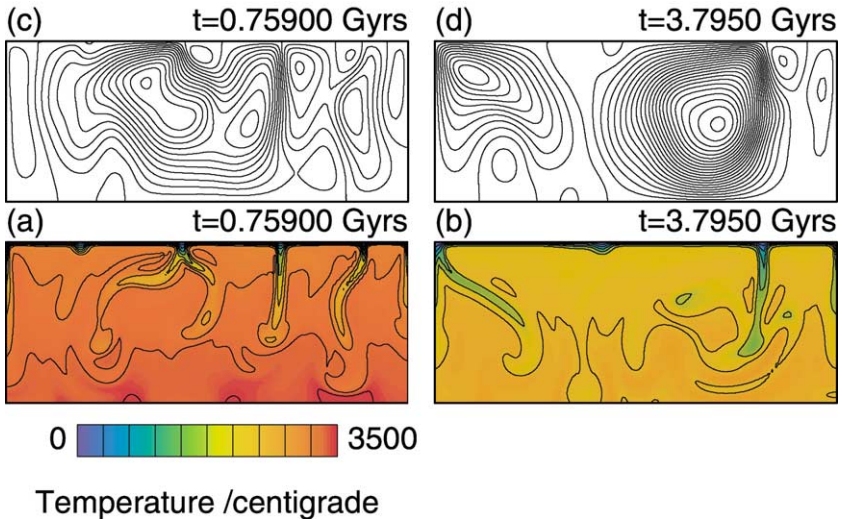

Fig. 2. Snapshots of the temperature field (bottom row), stream function (middle row), at two time instants far apart: $t = 0.76$ Gyr and $t = 3.8$ Gyr after the start of the model calculation. Results are for a constant conductivity model $k = 4.7$ W m^{-1} K^{-1}, for the same $Ra_s = 8 \times 10^6$ as in Fig. 1. The stream function contour spacing is 25 non-dimensional units. Velocity has been non-dimensionalized with respect to the thermal diffusivity.

study. In Fig. 2 we show the same fields for the constant conductivity case, starting from the same initial condition. There we note that the cooling process is faster with constant conductivity as shown by the lighter hue in the color. This phenomenon of greater degree of cooling is caused by the greater magnitudes of the downwellings and the deeper degree of penetration throughout the depth of the mantle, as shown by the concentration of the streamlines and their more complete circuits hitting the core–mantle boundary. Although the average Rayleigh number of the constant conductivity case (Fig. 2) is about a factor of 2 greater than that of variable conductivity (Fig. 1), there is more than a factor of 2 difference in the magnitude of the maximum downwelling velocities and a sharp difference in the style in the deeper penetration of the cold descending flow. Thus a distinct style of less penetrative flow is developed with variable conductivity, as the vertical symmetry is broken to a greater degree by the presence of $k(T,P)$.

In addition to the less efficient cooling by the more sluggish downwellings, the presence of a low thermal conductivity zone near the surface would trap the heat locally and would impede outward heat transfer from the rising currents, thus retarding the cooling rate. The occurrence of a low thermal conductivity zone, LCZ, at the top thermal boundary layer follows directly from the functional relationship of $k(T,P)$, given in Eq. 1. This LCZ phenomenon was first demonstrated by Schubert et al. [15] within the framework of a steady-state thermal–mechanical boundary layer modelling, using the thermal conductivity model by Schatz and Simmons [9], which had just the phonon contribution to the olivine conductivity. The presence of a LCZ was also shown in Hofmeister [7] for a conductive profile. In the 3-D thermal convection models without internal heating [19] the presence of two LCZs was also revealed in both the upper and lower mantle for a basally heated situation.

In Fig. 3 we display both the horizontally averaged temperature and conductivity profiles in the top 300 km of the mantle. These solutions have been integrated from the initial condition and two different surface Rayleigh numbers (8×10^6 and 1.6×10^7) at a time of 3.8 Gyr after the imposition of the initially hot state. Although the temperature profiles have dropped significantly from the initial profile by a factor close to 50%, the conductivity profiles reveal much smaller changes, less than 10%. But, as shown by Dubuffet et al.

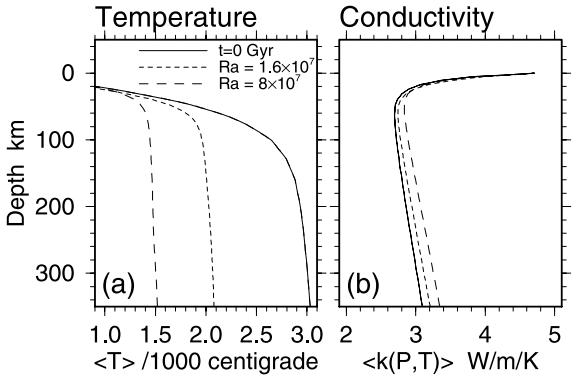

Fig. 3. Profiles of horizontally averaged temperature $T(z)$ (a) and thermal conductivity $k(z)$ for two Rayleigh numbers, 1.6×10^7, 8×10^7 and internal heating mode $R=20$. Solid lines show the initial T, k common to all models. Dashed lines correspond to the respective Rayleigh numbers at $t=3.8$ Gyr.

[22], the influence of variable conductivity can still be distinguished from the degree of thermal assimilation of the cold downwellings in 3-D high Rayleigh number convection at $Ra=7\times10^6$. Thus we should not underestimate the impact of variable thermal conductivity on the secular cooling process, on the basis of the relatively small change in the magnitudes of the thermal conductivity with time. Since the energy equation yields directly the dynamical timescales in pure thermal convection, small non-linearities in the diffusion equation, arising from the divergence term, can influence greatly the timescales from a mathematical standpoint [23].

In our model the rate of secular cooling depends critically on the following physically controlling factors, the surface Rayleigh number, the initial strength of radiogenic heating and the time of half-life of the radioactive decay. In Fig. 4 we focus on the differences in the global thermal evolution between constant (dashed lines) and variable (solid lines) thermal conductivity. We have monitored the temporal evolution of the volumetrically averaged temperature $\langle T\rangle$ in the spirit of parameterized convection models (e.g. [24]). We have plotted time logarithmically and this type of mapping reveals quite lucidly the multiple scale nature of the secular cooling process with time-dependent internal heating, first studied by Daly [25] with constant thermal conductivity. Besides the $f=1$ case, we have also considered the case with $f=5$, which would have a higher contribution of radiative heat transfer and a smaller effective Rayleigh number. In all cases the mantle cools slower with variable conductivity and $f=1$ (solid curves). The constant conductivity and the enhanced radiative conductivity ($f=5$) cases cool off faster and with nearly the same rate. There is very little difference between the two dashed curves ($f=5$) and constant conductivity. As expected, an increase of internal heating and a decrease in the convective vigor lengthen the time of cooling. The time of delay in the late stage of evolution is on the order of Gyr. Hence variable thermal conductivity with $f=1$ in a way acts in the same manner reminiscent of some sort of a barrier, as in partially layered convection induced by an endothermic phase transition and depth-dependence of mantle viscosity (e.g. [26,45]), or an enriched radiogenic heat source in the lower third of the mantle [27] in that the secular cooling in the

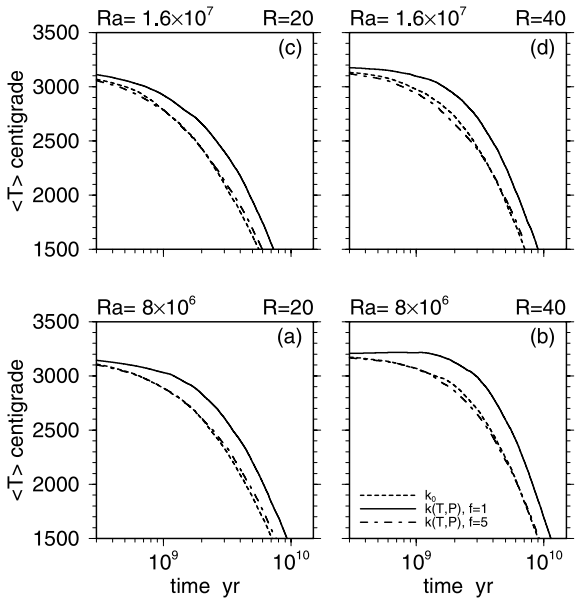

Fig. 4. Volume average temperature $\langle T\rangle$ versus t, for two Rayleigh numbers $Ra=8\times10^6$ (bottom frames) and $Ra=1.6\times10^7$ (top frames), and internal heating modes $R=20$ and 40. Three curves per frame correspond to different conductivity models, constant k (dotted), $k(T,P)$, $f=1$ (solid) and $k(T,P)$, $f=5$ (dashed). We note that $f=5$ has an enhanced radiative component in the thermal conductivity.

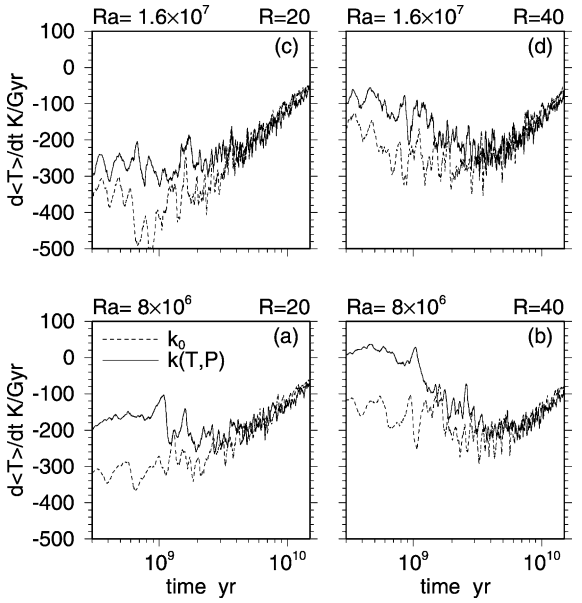

Fig. 5. Cooling rates $d\langle T\rangle/dt$ for each of the associated curves in Fig. 4. A seven-point box-car window has been applied to smooth out the derivative traces computed from central differencing the $\langle T(t)\rangle$ time series.

mantle would be delayed. Enhanced radiative transfer with $f=5$ would cool off the mantle faster than with $f=1$ and at a similar rate as that for constant conductivity. This paradox shows that one cannot use the concept of effective Rayleigh number in evaluating the efficiency of heat transfer with the presence of variable conductivity especially when a significant radiative component is included, since the effective Rayleigh number for $f=5$ is more than two times smaller than the effective Rayleigh number for constant conductivity and yet they have similar cooling rates, because radiative thermal conductivity makes up for this effective Rayleigh number. We will return to this point in Fig. 7.

The rate of global cooling is defined by the time derivative of the volumetrically averaged temperature, $d\langle T\rangle/dt$. This is an important quantity which is an output of parameterized convection models [28], described by the global energy balance equation:

$$C\frac{d\langle T\rangle}{dt} = Q(t) + I(t) \qquad (3)$$

where C is the total heat capacity of the mantle, $Q(t)$ is the surface heat-flux and $I(t)$ is the volume integrated internal heat production rate. We have computed $d\langle T\rangle/dt$ by central differencing the time series $\langle T(t)\rangle$, given at every integration time step [17]. This has been applied to the constant conductivity and the $f=1$ cases. We have applied a running box-car filter consisting of seven points to smoothen the resulting time series. The results for $d\langle T\rangle/dt$ corresponding to the cases shown in Fig. 4 are displayed in Fig. 5 with time again plotted on a logarithmic axis. The cooling rate appears to be a fluctuating quantity unlike the volume averaged temperature. This distinct feature, not found in parameterized convection models [24], arises from the fluctuating nature of the surface heat-flux term Q in Eq. 3, associated with the boundary layer instabilities and the global fluctuations in the Nusselt number characteristic of high Rayleigh number thermal convection [17,29]. The differences in the global rate are substantial in the first couple of billion years, with the constant conductivity models cooling faster by 100 K/Gyr in the first Gyr. We note that these are cartesian models and effects of sphericity would decrease the absolute cooling rates [30] by a factor of at least 2. Although these are constant viscosity models, we would expect the same trend for variable viscosity $\eta(T,P)$ models with variable conductivity $k(T,P)$ because of both the dominance of the cold downflows in the case of constant thermal conductivity and the enhanced decoupling of

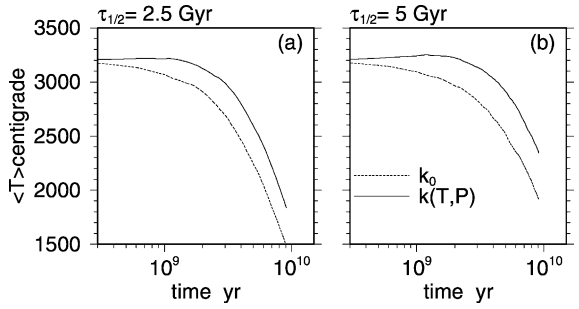

Fig. 6. Volume average temperature $\langle T\rangle$ versus t for $R=40$, $Ra=8\times10^6$ and two values of the radioactive half-life time of $\tau_{1/2}=2.5$ Gyr (a) and $\tau_{1/2}=5.0$ Gyr (b), for two conductivity models: constant k_0 and variable $k(T,P)$.

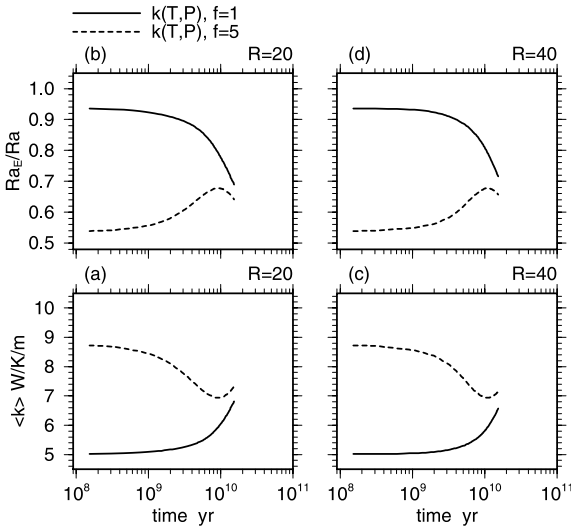

Fig. 7. Time series of volume averaged conductivity (a), (c), for a surface Rayleigh number $Ra = 1.6 \times 10^7$ and two internal heating modes $R = 20$ (a) and $R = 40$ (c). Solid curves are for a conductivity model with small radiative contribution ($f = 1$) and dashed curves are for a case with an enhanced radiative conductivity component ($f = 5$). The top frames (b), (d) show – for the same model cases as in (a) and (b) respectively – the ratio of the effective Rayleigh number Ra_E and the surface Rayleigh number, where Ra_E is based on the volumetrically averaged conductivity.

the low viscosity zone with the enhanced thermal perturbation of the low conductivity zone.

The effects of a longer half-life time on the secular cooling are illustrated in Fig. 6, where we have doubled the half-life time to 5 Gyr, which lie within plausible bounds in the rates of radioactive decay and effective concentration of the relevant radiogenic isotopes [3,31]. The initial value for R is 40, characteristic of an Archaean value of higher radioactivity and the surface Rayleigh number is set to 8×10^6. From Fig. 6a and b it is clear that a longer half-life time induces a longer period of delayed secular cooling.

We will now display in Fig. 7 the time history of the effective Rayleigh number Ra_E and the volumetrically averaged thermal conductivity $\langle k \rangle$. The effective Rayleigh number is defined here in terms of the volume average non-dimensional conductivity, $Ra_E = Ra/\langle k' \rangle$. These are presented for the two cases $f = 1$ and $f = 5$ in order to show that the usual argument of cooling timescale varying with $Ra^{-2/3}$ (e.g. [32]) is not valid with the presence of radiative thermal conductivity. In Fig. 4 we observed that the case for variable conductivity and $f = 1$ cools much slower than the cases for $f = 5$ and the constant conductivity cases. Yet in Fig. 7 for a surface Ra of around 1×10^7, we find that the averaged value $\langle Ra \rangle$ is lower for $f = 5$ than for $f = 1$ and also the averaged conductivity $\langle k \rangle$ for $f = 5$ is greater. This is due to the increased efficiency of the radiative mode of heat transfer at larger f value, thus invalidating the usual assumption that the Nusselt number is proportional to $Ra^{1/3}$ for constant thermal conductivity. This seemingly paradoxical result has also been found by van den Berg et al. [20] in their analysis of steady-state heat transfer for variable thermal

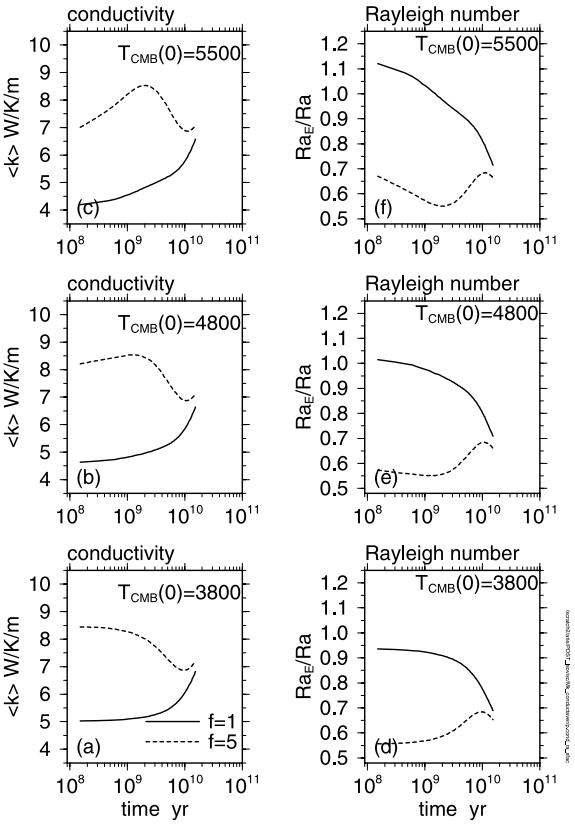

Fig. 8. Temporal evolution of the volume averaged conductivity and normalized Rayleigh number for three different initial temperatures at the core–mantle boundary. Solid curves are for a conductivity model with small radiative contribution ($f = 1$) and dashed curves are for a case with an enhanced radiative conductivity component ($f = 5$).

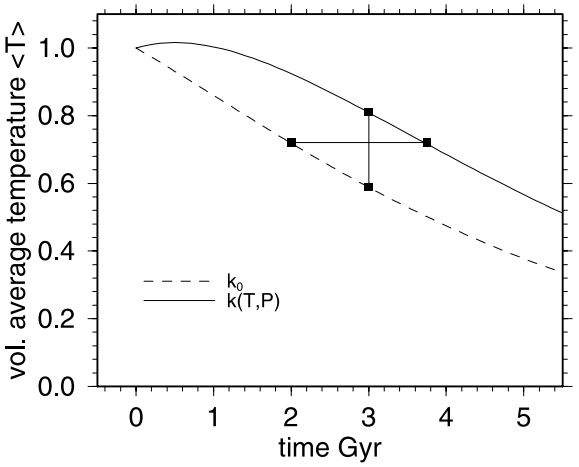

Fig. 9. Schematic diagram of mantle thermal evolution showing the time delay in secular cooling and the rise in the mantle temperature from variable thermal conductivity.

conductivity, in which the greatest Nusselt numbers were associated with the largest magnitude of temperature-dependent thermal conductivity, which was completely radiative in character, with $\partial k/\partial T$ being always positive. We further emphasize this paradoxical point by showing in Fig. 8 the evolution of $\langle k \rangle$ and the normalized Rayleigh number for higher initial temperatures at the CMB. The trajectory paths of $\langle k \rangle$ and normalized Rayleigh numbers are shown for the initial CMB temperatures of 3800, 4800 and 5500 K. Two values of f are used, $f = 1$ (solid curve) and $f = 5$ (dashed curve). At higher temperatures and $f = 5$ the non-linear interactions are so strong that non-monotonic behavior is developed in the $\langle k \rangle$ and Rayleigh number evolutionary curves. Usually in a cooling process one would expect the Rayleigh number to decay monotonically and not to exhibit a non-monotonic trend, as shown in the dashed curves of the right column. These results reveal the potential importance of the radiative component of thermal conductivity in thermal evolution of a young Earth when the interior was hotter than today's mantle.

In the Earth's interior many types of heating from the core with long timescale, such as Joule dissipation associated with geodynamo (e.g. [44]) or radiogenic heating from potassium [33] could act in concert with variable thermal conductivity and would therefore cause a greater delay in mantle cooling. The lower mantle might then become very hot because of both the inefficient upward transfer of heat in variable conductivity models [27], and this feedback process from radiogenic heating in direct analogy to the global warming of the atmosphere by CO_2 feedback (e.g. [34]). This scenario is portrayed schematically in Fig. 9, where we have displayed the sharp difference between the two evolutionary paths for mantle cooling with variable thermal conductivity (top curve) and one with constant thermal conductivity (bottom curve). We illustrate here the two important concepts, derived from this model: a delay in rate of cooling (horizontal bar) and a hotter mantle (vertical bar).

4. Concluding remarks

It has been well recognized that the mean global cooling rate of a planet depends on the initial mantle temperature, the radiogenic heat sources and the mode of heat transfer within the mantle. But the role of variable thermal conductivity in thermal evolution has been neglected for over 40 yr, since the initial work by Lubimova [35] and Mac Donald [36], who employed a radiatively dominant thermal conductivity within the framework of a non-linear heat diffusion equation with time-dependent radiogenic heating. In this connection, we note that one of the purposes of Lubimova and Mac Donald in employing a non-linear thermal conductivity was to slow down the cooling of the Earth from a purely thermal cooling model with constant conductivity from Lord Kelvin's early dilemma of having the Earth cooled down in less than 100 Myr [37]. Mac Donald [36] found that with radiative thermal conductivity he could delay the cooling of the Earth up to the order of couple billion years.

In this study we have investigated the effects of the secular cooling problem by 2-D convection simulations, which uses explicitly a thermal conductivity model based primarily on phonon dynamics with radiative contribution being minor [7]. Our results show unequivocally that this phonon-dominated thermal conductivity model because of the formation of the low conductivity

zone will cause a non-negligible delay in the secular cooling of the mantle, on the order of (Ga). This is caused by the formation of a low conductivity zone in the same manner as a low viscosity zone is formed by the temperature- and pressure-dependent trade-offs in the rheological constitutive relation. The same LCZ has been shown recently to be important for the production of long-living diapiric upwellings in the Martian mantle [38].

We have also shown that increasing the amount of radiative contribution will speed up the convective cooling process. Thus there exist certain regions in the parameter space of phonon versus photon heat transfer characteristics, where delayed cooling can conceivably take place. Our results presented here should be regarded as a lower bound, since we have employed an adiabatic boundary condition at the core–mantle boundary and have not taken an explicit thermal coupling of the mantle to the core (e.g. [5]) with both phonon and radiative thermal conductivity into account. The presence of a thermal boundary layer in the deep mantle would also produce another low conductivity zone just above the CMB [7,19], which would further impede the amount of heat transfer from the core. If there is more heat from the core than has been previously assumed from ohmic dissipation [39,40], then the problem of overheating in the lower mantle would further be exacerbated with the mechanical heat produced thermal-chemical convection [41] and an enriched heat distribution in the bottom 1000 km of the mantle [27]. Our work definitely argues for a reconsideration of the potentially important role played by variable thermal conductivity in the entire thermal history of the mantle and its interaction with core dynamics, since the heat transport in the present holds the key to the past thermal events, such as overheating in the lower mantle. Models of secular mantle and core cooling with constant conductivity (e.g. [42,43]) should be reevaluated with these remarks in mind.

Acknowledgements

We thank stimulating discussions with Drs. Anne M. Hofmeister, Arthur R. Calderwood, David Gubbins, Fabien Dubuffet, Don L. Turcotte and Volker Steinbach. We thank Jeff R. Allwardt for technical assistance. We acknowledge constructive reviews which helped improve the manuscript, by Louis Moresi and an anonymous reviewer. Support of this work has come from the geophysics program of the National Science Foundation.*[RV]*

References

[1] F.M. Flasar, F. Birch, Energetics of core formation: a correction, J. Geophys. Res. 78 (1973) 6101–6103.
[2] V.P. Keondjian, A.S. Monin, Model of gravitational differentiation of the planetary interiors, Dokl. Akad. Nauk. SSSR 220 (1975) 825–829.
[3] H.N. Pollack, Thermal characteristics of the Archaean, in: M.J. de Wit, L.D. Ashwal (Eds.), Greenstone Belts, Oxford University Press, Oxford, 1997, pp. 223–232.
[4] J.H. de Smet, A.P. van den Berg, N.J. Vlaar, Early formation and long-term stability of continents resulting from decompression melting in a convecting mantle, Tectonophysics 322 (2000) 19–33.
[5] V. Steinbach, D.A. Yuen, W. Zhao, Instabilities from phase transitions and the timescales of mantle evolution, Geophys. Res. Lett. 20 (1993) 1119–1122.
[6] A.P. van den Berg, D.A. Yuen, Convectively induced transition in mantle rheological behavior, Geophys. Res. Lett. 22 (1995) 1549–1552.
[7] A.M. Hofmeister, Mantle values of thermal conductivity and the geotherm from phonon lifetimes, Science 283 (1999) 1699–1706.
[8] A.M. Hofmeister, Thermal conductivity of spinels and olivines from vibrational spectroscopy at ambient conditions, Am. Mineral. 86 (2001) 1188–1208.
[9] J.F. Schatz, G. Simmons, Thermal conductivity of earth materials at high temperatures, J. Geophys. Res. 77 (1972) 6966–6983.
[10] J. Branlund, M.C. Kameyama, D.A. Yuen, Y. Kaneda, Effects of temperature-dependent thermal diffusivity on shear instability in a viscoelastic zone: Implication for faster ductile faulting and earthquakes in the spinel stability field, Earth Planet. Sci. Lett. 182 (2000) 171–185.
[11] A.P. van den Berg, D.A. Yuen, J.R. Allwardt, Nonlinear effects from variable thermal conductivity and mantle internal heating: Implications for massive melting and secular cooling of the mantle, Phys. Earth Planet. Inter., in press.
[12] F. Dubuffet, D.A. Yuen, E.S.G. Rainey, Controlling thermal chaos in the mantle by positive feedback from radiative thermal conductivity, Nonlinear Process, Geophys. 129 (2002) 359–375.

[13] A. Chopelas, R. Boehler, Thermal expansivity of the lower mantle, Geophys. Res. Lett. 19 (1992) 1983–1986.
[14] A.P. van den Berg, D.A. Yuen, Modelling planetary dynamics by using the temperature at the core-mantle boundary as a control variable effects of rheological layering on mantle heat transport, Phys. Earth Planet. Inter. 108 (1998) 219–234.
[15] G. Schubert, C. Froidevaux, D.A. Yuen, Oceanic lithosphere and asthenosphere: thermal and mechanical structure, J. Geophys. Res. 81 (1976) 3525–3541.
[16] V. Steinbach, U. Hansen, A. Ebel, Compressible convection in the earth's mantle: a comparison of different approaches, Geophys. Res. Lett. 16 (1989) 633–635.
[17] A.P. van den Berg, P.E. van Keken, D.A. Yuen, The effects of a composite non-Newtonian and Newtonian rheology in mantle convection, Geophys. J. Int. 115 (1993) 62–78.
[18] A. Leitch, D.A. Yuen, Internal heating and thermal constraints on the mantle, Geophys. Res. Lett. 16 (1989) 1407–1410.
[19] F. Dubuffet, D.A. Yuen, M. Rabinowicz, Effects of a realistic mantle thermal conductivity on the patterns of 3-D convection, Earth Planet. Sci. Lett. 171 (1999) 401–409.
[20] A.P. van den Berg, D.A. Yuen, V. Steinbach, The effect of variable thermal conductivity on mantle heat-transfer, Geophys. Res. Lett. 28 (2001) 875–878.
[21] P. Machetel, D.A. Yuen, Penetrative convective flows induced by internal heating and mantle compressibility, J. Geophys. Res. 94 (1989) 10609–10626.
[22] F. Dubuffet, D.A. Yuen, T. Yanagawa, Feedback effects of variable thermal conductivity on the cold downwellings in high Rayleigh number convection, Geophys. Res. Lett. 27 (2000) 2981–2984.
[23] P.L. Sachdev, Nonlinear Diffusive Waves, Cambridge University Press, Cambridge, 1987.
[24] G. Schubert, P. Cassen, R.E. Young, Subsolidus convective cooling histories of terrestrial planets, Icarus 38 (1979) 192–211.
[25] S.F. Daly, Convection with decaying heat sources: constant viscosity, Geophys. J. R. Astron. Soc. 61 (1980) 519–547.
[26] D.A. Yuen, D.M. Reuteler, S. Balachandar, V. Steinbach, A.V. Malevsky, J.J. Smedsmo, Various influences on three-dimensional mantle convection with phase transitions, Phys. Earth Planet. Inter. 86 (1994) 185–203.
[27] L.H. Kellogg, B.H. Hager, R.D. van der Hilst, Compositional stratification in the deep mantle, Science 283 (1999) 1881–1884.
[28] D.P. Mc Kenzie, N.O. Weiss, Speculations on the thermal and tectonic history of the Earth, Geophys. J. R. Astron. Soc. 42 (1975) 131–174.
[29] D.A. Yuen, U. Hansen, W. Zhao, A.P. Vincent, A.V. Malevsky, Hard turbulent thermal convection and thermal evolution of the mantle, J. Geophys. Res. 98 (E3) (1993) 5355–5373.
[30] Y. Iwase, S. Honda, Effects of geometry on the convection with core cooling, Earth Planets Space 50 (1998) 387–396.
[31] M.J. Jackson, H.N. Pollack, On the sensitivity of parameterized convection to the rate of decay of internal heat sources, J. Geophys. Res. 89 (B12) (1984) 10103–10108.
[32] H.N. Sharpe, W.R. Peltier, Parameterized mantle convection and the Earth's thermal history, Geophys. Res. Lett. 5 (1978) 737–740.
[33] D. Breuer, T. Spohn, Cooling of the Earth, Urey ratios, and the problem of potassium in the core, Geophys. Res. Lett. 20 (1993) 1655–1658.
[34] P.J. Sellers, L. Bounoua, G.J. Collatz et al., Comparison of radiative and physiological effects of doubled atmospheric CO_2 on climate, Science 271 (1996) 1402–1405.
[35] H. Lubimova, Thermal history of the earth with consideration of the variable thermal conductivity of the mantle, Geophys. J. R. Astron. Soc. 1 (1958) 115–134.
[36] G.J.F. Mac Donald, Calculations on the thermal history of the earth, J. Geophys. Res. 64 (1959) 1967–2000.
[37] F.M. Richter, Kelvin and the age of the earth, J. Geol. 94 (1986) 395–401.
[38] B. Schott, A.P. van den Berg, D.A. Yuen, Focussed time-dependent Martian volcanism from chemical differentiation coupled with variable thermal conductivity, Geophys. Res. Lett. 28 (2001) 4271–4274.
[39] A.R. Calderwood, The magnitude and efficiency of the power sources driving the geodynamo and the age of the inner core, American Geophysical Union, Fall Abstract, 2000.
[40] P.H. Roberts, C.A. Jones, A. Calderwood, Energy fluxes and Ohmic dissipation in the Earth's core, in: A.M. Soward, C.A. Jones, K. Zhang (Eds.), Earth's Core and Lower Mantle, Gordon and Breach, London, to appear.
[41] U. Hansen, D.A. Yuen, Extended-Boussinesq thermal-chemical convection with moving heat sources and variable viscosity, Earth Planet. Sci. Lett. 176 (2000) 401–411.
[42] S. Labrosse, J.P. Poirier, J.L. LeMouel, On cooling of the Earth's core, Phys. Earth Planet. Inter. 99 (1997) 1–17.
[43] G. Choblet, C. Sotin, 3D thermal convection with variable viscosity: can transient cooling be described by a quasi-static scaling law?, Phys. Earth Planet. Inter. 119 (2000) 321–336.
[44] D. Gubbins, T.G. Masters, J.A. Jacobs, Thermal evolution of the Earth's core, Geophys. J. R. Astron. Soc. 59 (1979) 57–79.
[45] S.L. Butler, W.R. Peltier, The Thermal evolution of the Earth: models with time-dependent layering of mantle convection which satisfy the Urey ratio constraint, J. Geophys. Res., in press.